J|A|C|S
ARTICLES
Published on Web 01/13/2007

Structure of Molecular Tweezer Complexes in the Solid State: NMR Experiments, X-ray Investigations, and Quantum Chemical Calculations

Torsten Schaller,*,† Uta P. Büchele,† Frank-Gerrit Klärner,† Dieter Bläser,† Roland Boese,† Steven P. Brown,‡ Hans Wolfgang Spiess,§ Felix Koziol,|| Jörg Kussmann,⊥ and Christian Ochsenfeld⊥

Contribution from the Universität Duisburg-Essen, Institut für Organische Chemie, D-45117 Essen, Germany, Department of Physics, University of Warwick, Coventry, CV4 7AL, United Kingdom, Max-Planck-Institut für Polymerforschung, Postfach 3148, D-55021 Mainz, Germany, Department of Chemistry and Chemical Biology, Harvard University, Cambridge, Massachusetts 02138, and Universität Tübingen, Institut für Physikalische und Theoretische Chemie, Auf der Morgenstelle 8, D-72076 Tübingen, Germany

Received September 14, 2006; E-mail: torsten.schaller@uni-due.de

Abstract: The structure of supramolecular complexes formed by a naphthalene-spaced tweezer molecule as host and 1,4-dicyanobenzene (DCNB), 1,2,4,5-tetracyanobenzene (TCNB), and 7,7,8,8-tetracyano-*p*-quinodimethane (TCNQ) as aromatic, electron-deficient guests is investigated by solid-state NMR and X-ray diffraction measurements. Quantum chemical calculations using linear scaling methods are applied to predict and to assign the ^{1}H NMR chemical shifts of the complexes. By combining experiment and theory, insights into intra- and intermolecular effects influencing the proton chemical shifts of the host−guest system are provided in the solid state.

1. Introduction

Studies on the structure and the functionality of natural receptors often face difficulties due to the size and complexity of the objects of interest. Therefore, much insight can be gained by investigating the interactions between substrate and receptor in rather simple model systems.[1−3] Of considerable interest are supramolecular complexes formed by noncovalent interactions such as the ubiquitous hydrogen bonding,[4] ion pairing,[5] and arene−arene interactions[6−9] which are known to have significant influence on the formation and structure of complexes between natural receptors and various ligands.

Many model receptors (for example, the macrocyclic cyclodextrins[10] or cyclophanes[11]) have a predefined, rather rigid structure, whereas noncyclic receptors named molecular tweezers and clips[12−17] are compounds having a well preorganized yet flexible shape enabling variation in the size of the binding site.

It has been shown that such tweezers and clips form complexes with electron-deficient aromatic and aliphatic guest molecules,[18] as well as inorganic and organic cations (for example, NAD^+).[19,20] This selectivity has been explained in terms of an interplay of electrostatic interactions between the receptor and the substrate and attractive CH−π and $\pi-\pi$ interactions.[21]

Complexes formed by a wide variety of such ribbon-shaped receptors and a suite of various substrate molecules have been investigated using solution state NMR, calorimetric measurements, and optical spectroscopy (UV/vis, fluorescence measurements).[21] Information about the structure and thermodynamic

† Universität Duisburg-Essen.
‡ University of Warwick.
§ Max-Planck-Institut für Polymerforschung.
|| Harvard University.
⊥ Universität Tübingen.

(1) Lehn, J. M. *Supramolecular Chemistry Concepts and Perspectives*; VCH: Weinheim, 1995.
(2) Schneider, H.-J.; Yatsimirsky, A. *Principles and Methods in Supramolecular Chemistry*; Wiley-VCH: Weinheim, 2000.
(3) Atwood, J. L.; Steed, J. W. *Supramolecular Chemistry*; WILEY: Weinheim, 2000.
(4) Prins, L. J.; Reinhoudt, D. N.; Timmerman, P. *Angew. Chem., Int. Ed.* **2001**, *40*, 2383−2426.
(5) Gallivan, J. P.; Dougherty, D. A. *J. Am. Chem. Soc.* **2000**, *122*, 870−874.
(6) Hunter, C. A.; Lawson, K. R.; Perkins, J.; Urch, C. J. *J. Chem. Soc., Perkin Trans. 2* **2001**, 651−669.
(7) Kim, E.; Paliwal, S.; Wilcox, C. S. *J. Am. Chem. Soc.* **1998**, *120*, 11192−11193.
(8) Meyer, E. A.; Castellano, R. K.; Diederich, F. *Angew. Chem., Int. Ed.* **2003**, *42*, 1210−1250.
(9) Sinnokrot, M. O.; Valeev, E. F.; Sherrill, C. D. *J. Am. Chem. Soc.* **2002**, *124*, 10887−10893.
(10) Rekharsky, M. V.; Inoue, Y. *Chem. Rev.* **1998**, *98*, 1875−1917.
(11) Diederich, F. *Cyclophanes*; Royal Society of Chemistry: Cambridge, 1991.
(12) Chen, C. W.; Whitlock, H. W., Jr. *J. Am. Chem. Soc.* **1978**, *100*, 4921−2.
(13) Zimmerman, S. C.; VanZyl, C. M.; Hamilton, G. S. *J. Am. Chem. Soc.* **1989**, *111*, 1373−81.
(14) Zimmerman, S. C. *Top. Curr. Chem.* **1993**, *165*, 71−102.
(15) Rowan, A. E.; Elemans, J.; Nolte, R. J. M. *Acc. Chem. Res.* **1999**, *32*, 995−1006.
(16) Klärner, F.-G.; Benkhoff, J.; Boese, R.; Burkert, U.; Kamieth, M.; Naatz, U. *Angew. Chem., Int. Ed. Engl.* **1996**, *35*, 1130−1133.
(17) Klärner, F.-G.; Panitzky, J.; Bläser, D.; Boese, R. *Tetrahedron* **2001**, *57*, 3673−3687.
(18) Klärner, F.-G.; Burkert, U.; Kamieth, M.; Boese, R.; Benet-Buchholz, J. *Chem.−Eur. J.* **1999**, *5*, 1700−1707.
(19) Jasper, C.; Schrader, T.; Panitzky, J.; Klärner, F.-G. *Angew. Chem., Int. Ed.* **2002**, *41*, 1355−1358.
(20) Klärner, F.-G.; Burkert, U.; Kamieth, M.; Boese, R. *J. Phys. Org. Chem.* **2000**, *13*, 604−611.
(21) Klärner, F. G.; Kahlert, B. *Acc. Chem. Res.* **2003**, *36*, 919−932.

and kinetic stability of these complexes in solution (organic solvents and water) has been obtained from experimental data in combination with molecular modeling and quantum-chemical studies.[22] In particular, the position of the guest molecule within the receptor cavity and, in some prominent cases, the deformation of the receptor geometry[23] resulting from complex formation were elucidated either from single-crystal studies or by the combination of quantum-chemical NMR shift calculations with experimental studies (vide infra). In addition, dynamic processes can be monitored:[24] the association/dissociation of the complexes and periodic motions of the guest molecule within the cavity of the receptor strongly depend on the chosen solvent, the host/guest concentration, and the temperature. The time scale of these processes can be estimated, and the Gibbs free enthalpy of activation $\Delta G^{\#}$ can be determined. The stability of the complexes formed is usually characterized by the association constant K_a determined by NMR titration experiments for $K_a \leq 10^5$ and calorimetric/fluorometric measurements for $K_a > 10^5$. While, the complexes are usually studied in solution (in organic solvents or water), a recent mass spectrometry study now demonstrated for the first time the stability of complexes formed by a naphthalene-spaced tweezers and dendritic viologene salts in the gas phase.[25]

Experimentally, it has also been found that a number of complexes, in particular those with a rather large association constant, tend to crystallize and form single crystals or, at least, a polycrystalline powder. Single-crystal structure data are available for pure complexes and complexes incorporating solvent molecules such as chloroform or methylene chloride within the crystal lattice whereby the solvent molecules influence the spatial arrangement of the host−guest complexes.[18]

In the solid state, the study of the interaction between receptor and substrate is, on one hand, simplified by the fact that the guest molecule remains complexed and positioned within the cavity, thus allowing a more direct investigation of the host−guest interactions. On the other hand, sophisticated solid-state NMR techniques are needed to extract structural information from poorly resolved spectra. As shown by numerous solution state NMR experiments,[21] a key highly sensitive parameter is the ^{1}H isotropic chemical shift (in particular those of the guest molecules). Depending on their geometrical arrangement, the guest protons are shielded due to the ring currents associated with adjacent host arene units resulting in high field shifts (up to 6 ppm).[26] In order to be able to monitor these shifts also in the solid state, the spectral resolution has to be enhanced by line narrowing techniques.

Nowadays, fast magic-angle spinning (MAS) NMR with spinning frequencies of at least 30 kHz is becoming a routine method to investigate solid samples, with the resolution so obtained in ^{1}H NMR spectra often being sufficient to resolve distinct important resonances.[27] Other methods are based on a combination of the physical rotation of the sample by MAS with pulse sequences that rotate the ^{1}H spins in spin space, thus further reducing the line broadening due to the strong and extensive dipolar interactions among the protons.[28] Recently, methods such as phase/frequency-modulated implementations of the Lee−Goldburg experiment[29−33] as well as the DUMBO[34,35] approach are being intensively investigated and applied in two-dimensional homonuclear[36−40] and heteronuclear[41−45] experiments.

While, on the one hand, high resolution in ^{1}H solid-state NMR requires the removal of the broadening due to the dipolar coupling, on the other hand, the dipolar couplings depend on the distances between the spins and thus provide important structural information. An elegant way to access this information without losing the advantages of fast MAS is ^{1}H double-quantum (DQ) spectroscopy.[27,46−48] In such a two-dimensional experiment, double quantum coherences due to pairs of dipolar coupled protons (the double-quantum chemical shift is the sum of the single-quantum chemical shifts) are correlated with single-quantum coherences resulting in correlation peaks characteristic for ^{1}H−^{1}H pairs. Like and unlike spins can easily be distinguished: they appear as a single correlation peak on the $F1 = 2 \cdot F2$ diagonal and a pair of cross-peaks symmetrically arranged either side of the diagonal, respectively. ^{1}H double-quantum (DQ) spectroscopy has been successfully applied to a wide range of different applications such as structural and dynamic studies for inter- and intramolecular hydrogen bonding,[49−51] water of crystallization in inorganic crystals,[52] polymeric systems,[53−57]

(22) Fokkens, M.; Jasper, C.; Schrader, T.; Koziol, F.; Ochsenfeld, C.; Polkowska, J.; Lobert, M.; Kahlert, B.; Klärner, F.-G. *Chem.−Eur. J.* **2005**, *11*, 477−494.
(23) Klärner, F.-G.; Kahlert, B.; Boese, R.; Blaser, D.; Juris, A.; Marchioni, F. *Chem.−Eur. J.* **2005**, *11*, 3363−3374.
(24) Lobert, M.; Bandmann, H.; Burkert, U.; Büchele, U. P.; Podsadlowski, V.; Klärner, F.-G. *Chem.−Eur. J.* **2006**, *12*, 1629−1641.
(25) Schalley, C. A.; Verhaelen, C.; Klärner, F.-G.; Hahn, U.; Vögtle, F. *Angew. Chem., Int. Ed.* **2005**, *44*, 477−480.
(26) Lazzeretti, P. *Prog. Nucl. Magn. Reson. Spectrosc.* **2000**, *36*, 1−88.
(27) Brown, S. P.; Spiess, H. W. *Chem. Rev.* **2001**, *101*, 4125−4155.
(28) Mehring, M. *Principles of high-resolution NMR in solids*, 2nd ed.; Springer-Verlag: Berlin; New York, 1983.
(29) Lee, M.; Goldburg, W. I. *Phys. Rev. A* **1965**, *140*, 1261−1271.
(30) Madhu, P. K.; Vinogradov, E.; Vega, S. *Chem. Phys. Lett.* **2004**, *394*, 423−428.
(31) Vega, A. J. *J. Magn. Reson.* **2004**, *170*, 22−41.
(32) Bosman, L.; Madhu, P. K.; Vega, S.; Vinogradov, E. *J. Magn. Reson.* **2004**, *169*, 39−48.
(33) Bielecki, A.; Kolbert, A. C.; Levitt, M. H. *Chem. Phys. Lett.* **1989**, *155*, 341−6.
(34) Sakellariou, D.; Lesage, A.; Hodgkinson, P.; Emsley, L. *Chem. Phys. Lett.* **2000**, *319*, 253−260.
(35) Lesage, A.; Sakellariou, D.; Hediger, S.; Elena, B.; Charmont, P.; Steuernagel, S.; Emsley, L. *J. Magn. Reson.* **2003**, *163*, 105−113.
(36) Lesage, A.; Duma, L.; Sakellariou, D.; Emsley, L. *J. Am. Chem. Soc.* **2001**, *123*, 5747−5752.
(37) Vinogradov, E.; Madhu, P. K.; Vega, S. *Chem. Phys. Lett.* **1999**, *314*, 443−450.
(38) Brown, S. P.; Lesage, A.; Elena, B.; Emsley, L. *J. Am. Chem. Soc.* **2004**, *126*, 13230−13231.
(39) Elena, B.; de Paepe, G.; Emsley, L. *Chem. Phys. Lett.* **2004**, *398*, 532−538.
(40) Elena, B.; Emsley, L. *J. Am. Chem. Soc.* **2005**, *127*, 9140−9146.
(41) van Rossum, B. J.; de Groot, C. P.; Ladizhansky, V.; Vega, S.; de Groot, H. J. M. *J. Am. Chem. Soc.* **2000**, *122*, 3465−3472.
(42) van Rossum, B. J.; Castellani, F.; Pauli, J.; Rehbein, K.; Hollander, J.; de Groot, H. J. M.; Oschkinat, H. *J. Biomol. NMR* **2003**, *25*, 217−223.
(43) Lesage, A.; Charmont, P.; Steuernagel, S.; Emsley, L. *J. Am. Chem. Soc.* **2000**, *122*, 9739−9744.
(44) Lesage, A.; Sakellariou, D.; Steuernagel, S.; Emsley, L. *J. Am. Chem. Soc.* **1998**, *120*, 13194−13201.
(45) Yates, J. R.; Pham, T. N.; Pickard, C. J.; Mauri, F.; Amado, A. M.; Gil, A. M.; Brown, S. P. *J. Am. Chem. Soc.* **2005**, *127*, 10216−10220.
(46) Geen, H.; Titman, J. J.; Gottwald, J.; Spiess, H. W. *Chem. Phys. Lett.* **1994**, *227*, 79−86.
(47) Gottwald, J.; Demco, D. E.; Graf, R.; Spiess, H. W. *Chem. Phys. Lett.* **1995**, *243*, 314−323.
(48) Schnell, I.; Spiess, H. W. *J. Magn. Reson.* **2001**, *151*, 153−227.
(49) Schnell, I.; Brown, S. P.; Low, H. Y.; Ishida, H.; Spiess, H. W. *J. Am. Chem. Soc.* **1998**, *120*, 11784−11795.
(50) Brown, S. P.; Zhu, X. X.; Saalwachter, K.; Spiess, H. W. *J. Am. Chem. Soc.* **2001**, *123*, 4275−4285.
(51) Brown, S. P.; Schnell, I.; Brand, J. D.; Müllen, K.; Spiess, H. W. *Phys. Chem. Chem. Phys.* **2000**, *2*, 1735−1745.
(52) Alam, T. M.; Nyman, M.; Cherry, B. R.; Segall, J. M.; Lybarger, L. E. *J. Am. Chem. Soc.* **2004**, *126*, 5610−5620.
(53) Spiess, H. W. *J. Polym. Sci., Part A: Polym. Chem.* **2004**, *42*, 5031−5044.
(54) Saalwachter, K.; Ziegler, P.; Spyckerelle, O.; Haidar, B.; Vidal, A.; Sommer, J. U. *J. Chem. Phys.* **2003**, *119*, 3468−3482.

columnar liquid-crystalline phases exhibiting $\pi-\pi$ packing,[58,59] and the inclusion of small molecules in nanochannels[56] and nanotubes.[60]

The extraction of structural and dynamic information from ^{1}H DQ MAS spectra depends on the assignment of the ^{1}H chemical shifts. As shown in recent publications investigating hexabenzocoronene systems, molecular tweezers, molecular clips,[61−65] and a penicillin salt,[66] the calculation of chemical shifts using quantum-chemical methods is invaluable in allowing reliable assignments of the experimental data. In this way it is possible to attain new insights into structural arrangements in both solution and the solid state. Indeed, the power of a combined experimental and computational approach is being increasingly recognized[45,66−70] and applied in the growing field of "NMR crystallography"[67,71,72] where inter- and intramolecular ^{1}H−^{1}H distances[40] or ^{1}H chemical shifts[73] are used as input for computational methods. Notably, with the development of new quantum chemical methods for the calculation of NMR shieldings at both Hartree−Fock (HF) and Density Functional Theory (DFT) level, the scaling of the computational effort with respect to the molecular size was recently demonstrated to be reduced to linear.[65] These methods allow molecular systems with more than 1000 atoms to be studied, so that not only can large molecules be investigated but also the study of molecules within their extended environment becomes possible in solution or in the solid state. Moreover, recent work allows the prefactors of the computational effort to be reduced even further by using new multipole-based integral estimates (MBIE) for two-electron integrals, thus accounting for the $1/R$ distance decay .[74,75]

In earlier studies,[63,64] we have successfully combined solid-state NMR experiments with quantum chemical calculations, together with data from X-ray diffraction experiments, in order to study the host−guest complex formed by a naphthalene-spaced tweezer with 1,4-dicyanobenzene (DCNB) as guest molecule (see Figure 1).

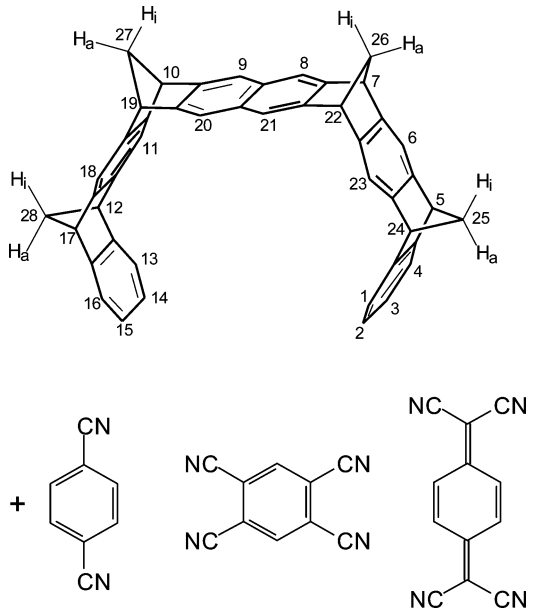

Figure 1. Naphthalene-spaced tweezer and guest molecules 1,4-dicyanobenzene (DCNB), 1,2,4,5-tetracyanobenzene (TCNB), and 7,7,8,8-tetracyano-*p*-quinodimethane (TCNQ).

Specifically, the guest and tweezer ^{1}H chemical shifts were assigned using ^{1}H DQ NMR spectroscopy as well as ^{1}H−^{13}C REPT-HSQC NMR heteronuclear correlation experiments.[76] In addition, both ^{1}H and ^{13}C chemical shifts were computed, thus allowing the influences on the chemical shifts (i.e., influences arising from within one and the same host−guest complex or from neighboring complexes) to be distinguished,[64] with these effects being particularly strong due to the arene ring current effects. The results demonstrated that the ^{1}H chemical shift is a highly sensitive probe of changes not only within the complex structure but also with respect to the solid-state environment.

This latter aspect is one of the main focuses of the present paper. Besides the complexation-induced chemical shift of the guest protons, the ^{1}H chemical shifts of the tweezer protons have been calculated for complexes with different packing schemes in the crystal lattice. In particular, it will be shown that the application of conventional as well as the recently developed linear-scaling techniques[65] provides ^{1}H chemical shifts which are in very good agreement with the NMR results. Moreover, it was possible to compute large fragments of the solid-state structure (up to 490 atoms). Results on complexes with three specific guest molecules will be presented: 1,4-dicyanobenzene (DCNB), 1,2,4,5-tetracyanobenzene (TCNB), and 7,7,8,8-tetracyano-*p*-quinodimethane (TCNQ).

2. Methodological Details

2.1. Experimental Details. The synthesis of the tweezer and its complexes is described elsewhere.[18] It should be noted that we could not obtain single crystals suitable for X-ray studies for the tweezer alone. As found in many similar systems (such as tri- and dimethylene bridged clips), these receptors often need to be stabilized in the solid state by guest or solvent molecules (such as chloroform, methylene chloride, and methanol). The host−guest samples investigated in this study do not suffer from solvent molecules incorporated in the crystal lattice.

(55) Saalwachter, K. *J. Chem. Phys.* **2004**, *120*, 454−464.
(56) Becker, J.; Comotti, A.; Simonutti, R.; Sozzani, P.; Saalwachter, K. *J. Phys. Chem. B* **2005**, *109*, 23285−23294.
(57) Rapp, A.; Schnell, I.; Sebastiani, D.; Brown, S. P.; Percec, V.; Spiess, H. W. *J. Am. Chem. Soc.* **2003**, *125*, 13284−13297.
(58) Brown, S. P.; Schnell, I.; Brand, J. D.; Müllen, K.; Spiess, H. W. *J. Am. Chem. Soc.* **1999**, *121*, 6712−6718.
(59) Brown, S. P.; Schnell, I.; Brand, J. D.; Müllen, K.; Spiess, H. W. *J. Mol. Struct.* **2000**, *521*, 179−195.
(60) Hoffmann, A.; Sebastiani, D.; Sugiono, E.; Yun, S.; Kim, K. S.; Spiess, H. W.; Schnell, I. *Chem. Phys. Lett.* **2004**, *388*, 164−169.
(61) Ochsenfeld, C. *Phys. Chem. Chem. Phys.* **2000**, *2*, 2153−2159.
(62) Ochsenfeld, C.; Brown, S. P.; Schnell, I.; Gauss, J.; Spiess, H. W. *J. Am. Chem. Soc.* **2001**, *123*, 2597−2606.
(63) Brown, S. P.; Schaller, T.; Seelbach, U. P.; Koziol, F.; Ochsenfeld, C.; Klärner, F.-G.; Spiess, H. W. *Angew. Chem., Int. Ed.* **2001**, *40*, 717−720.
(64) Ochsenfeld, C.; Koziol, F.; Brown, S. P.; Schaller, T.; Seelbach, U. P.; Klärner, F.-G. *Solid State Nucl. Magn. Reson.* **2002**, *22*, 128−153.
(65) Ochsenfeld, C.; Kussmann, J.; Koziol, F. *Angew. Chem., Int. Ed.* **2004**, *43*, 4485−4489.
(66) Harris, R. K.; Joyce, S. A.; Pickard, C. J.; Cadars, S.; Emsley, L. *Phys. Chem. Chem. Phys.* **2006**, *8*, 137−143.
(67) Harris, R. K. *Solid State Sci.* **2004**, *6*, 1025−1037.
(68) Potrzebowski, M. J.; Assfeld, X.; Ganicz, K.; Olejniczak, S.; Cartier, A.; Gardiennet, C.; Tekely, P. *J. Am. Chem. Soc.* **2003**, *125*, 4223−4232.
(69) Strohmeier, M.; Grant, D. M. *J. Am. Chem. Soc.* **2004**, *126*, 966−977.
(70) Strohmeier, M.; Stueber, D.; Grant, D. M. *J. Phys. Chem. A* **2003**, *107*, 7629−7642.
(71) Dutour, J.; Guillou, N.; Huguenard, C.; Taulelle, F.; Mellot-Draznieks, C.; Ferey, G. *Solid State Sci.* **2004**, *6*, 1059−1067.
(72) Taulelle, F. *Solid State Sci.* **2004**, *6*, 1053−1057.
(73) Harris, R. K.; Ghi, P. Y.; Hammond, R. B.; Ma, C. Y.; Roberts, K. J. *Chem. Commun.* **2003**, 2834−2835.
(74) Lambrecht, D. S.; Ochsenfeld, C. *J. Chem. Phys.* **2005**, *123*, 184101.
(75) Lambrecht, D. S.; Doser, B.; Ochsenfeld, C. *J. Chem. Phys.* **2005**, *123*, 184102.
(76) Saalwachter, K.; Graf, R.; Spiess, H. W. *J. Magn. Reson.* **1999**, *140*, 471−476.

Solution-state NMR spectra were recorded on a BRUKER DRX 500 spectrometer with a proton Larmor frequency of 500.1 MHz. All solid-state NMR experiments were performed on a standard-bore BRUKER DRX 700 spectrometer, operating at Larmor frequencies of 700.1 MHz (^{1}H) and 176.1 MHz (^{13}C). 10 mg of sample (no isotope enrichment) were rotated in a 2.5 mm MAS probe at a spinning frequency of 30 kHz. All experiments used 90° pulses of 2.0 μs and recycle delays of 1.0 s.

The back-to-back pulse sequence[47] was applied to excite and reconvert the double quantum coherences in the ^{1}H DQ MAS experiment. For each of 64 t_1 slices 16 transients were coadded. The ^{1}H−^{13}C correlation spectrum was recorded using the REPT-HSQC technique[76] employing a REDOR-type recoupling[77] for the heteronuclear polarization transfer. For each of 24 t_1 slices 1024 transients were coadded. In all two-dimensional experiments, the increment in t_1 was set to one rotor period, and sign discrimination was achieved using the States method.

2.2. Quantum-Chemical Calculations. Ab initio calculations were carried out using the program packages Q-Chem[78] and TURBOMOLE.[79] Structure optimizations were performed using linear scaling methods as implemented in the Q-Chem program: for the Hartree−Fock (HF) method, the linear exchange method LinK (linear exchange K) has been used,[80,81] whereas, for the Coulomb part, multipole expansions were employed (CFMM; continuous fast multipole method).[82,83] The numerical accuracy and reliability of these methods is exactly the same as that of conventional ab initio methods, except that the asymptotic scaling of the computational effort is reduced to linear for molecules with a nonvanishing HOMO−LUMO gap. For the CFMM method the linear scaling is achieved regardless of the HOMO−LUMO gap.

All structure optimizations presented in this study were performed at the HF/6-31G* level. The accuracy of HF/6-31G* structural parameters as a basis for the calculation of NMR chemical shifts has been discussed elsewhere[61,62] and can be estimated to yield proton chemical shifts with an accuracy of typically 0.2−0.4 ppm.

NMR chemical shifts were calculated using gauge-including atomic orbitals (GIAO)[84] at the HF level (GIAO-HF).[85−87] Most chemical shifts were computed with the program system TURBOMOLE[79] prior to our new development of a linear-scaling method for the calculation of NMR shieldings[65] implemented in the Q-Chem package. The new linear-scaling technique for NMR chemical shifts was then used for the largest solid-state fragment computed in this work consisting of five host−guest complexes (490 atoms). All chemical shifts are given in ppm relative to the commonly used TMS (tetramethylsilane) standard; the structure and chemical shifts of the considered molecular system and TMS are always computed at the same level of theory to allow for a balanced treatment. The monomer (one host−guest complex) values shown in Table 1 for the chemical shifts were computed at the GIAO-HF/TZP and GIAO-HF/6-31G* level, respectively. The calculations for the larger fragments are described below.

2.3. Crystallographic Data of the Complex with TCNB. A yellow crystal with the plate shaped approximate dimensions 0.36 × 0.28 × 0.08 mm^3 was measured at 203 K on a Siemens SMART diffractometer with a Bruker Apex II detector. With the formula weight 762.87 Da ($C_{46}H_{32}\cdot C_{10}H_2N_4$) the density is 1.267 g cm^{-3} for $Z = 4$ in a monoclinic unit cell (a = 15.075(2) Å, b = 10.6460(15) Å, c = 24.925(4) Å, β = 91.351(3)°, V = 3999.2(10) Å^3) in space group $C2/c$, which implies molecular C_2 symmetry. 29 434 intensities were collected; 2749 ($F_o \geq 2\sigma$) of the 4968 independent intensities [R(int) = 0.0594] were used. Crystal structure solution by Direct Methods and refinement on F^2 were performed using the Bruker AXS SHELXTL Vers. 5.10 software suite after data reduction, and empirical absorption correction was performed using Bruker AXS SAINT program Vers. 6.0. With hydrogen atoms treated as riding groups and all other atoms with ADPs (271 parameter), the refinement converged at $R1$ = 0.0538 and $wR2$ = 0.1264 (all data), and the residual electron density is 0.297 and −0.187 e Å^{-3}. CCDC-618377 contains the supplementary crystallographic data for this paper. These data can be obtained free of charge via www.ccdc.cam.ac.uk/conts/retrieving.html (or from the Cambridge Crystallographic Data Centre, 12 Union Road, Cambridge CB2 1EZ, UK; fax: (+44)1223-336-033; or e-mail: deposit@ccdc.cam.ac.uk).

Table 1. Chemical Shifts

	^{1}H chemical shift [ppm] from			
position	solution state NMR[a]	solid-state NMR	ab initio calculations	ab initio calculations
1,4-dicyanobenzene (DCNB)			monomer[b]	trimer[c]
H_{arom}	6.98−7.17	7.0−7.1	7.1−8.0	6.7−7.9
$H_{arom,term}$	6.36	5.0	6.5	4.9
$H_{bridgehead}$	4.11; 4.13	3.8	3.9−4.2	3.0−4.2
$H_{methylene}$	2.39−2.50	−1.2; 2.0	2.0−2.3	−0.4−2.4
$H_{guest,a}$	3.50	2.0	1.7	1.4
$H_{guest,b}$	3.50	5.6	5.3	4.9
1,2,4,5-tetracyanobenzene (TCNB)			monomer[b]	dimer[d]
H_{arom}	7.05−7.49	6.8−7.0	7.3−8.0	7.0−7.7
$H_{arom,term}$	6.28	4.9	6.6	4.9
$H_{bridgehead}$	4.23; 4.32	3.7	4.1−4.2	3.4−4.0
$H_{methylene}$	2.40−2.47	−0.1; 1.4	2.0−2.3	−1.0−2.2
H_{guest}	2.00	1.8	1.7	1.2
7,7,8,8-tetracyano-*p*-quinodimethane (TCNQ)			monomer[e]	pentamer[e]
H_{arom}	6.97−7.31	6.8	7.2−7.8	6.0−7.6
$H_{arom,term}$	6.36	5.7	6.6−7.0	6.7−7.3
$H_{bridgehead}$	4.16; 4.20	2.9	3.9−4.1	2.8−4.2
$H_{methylene}$	2.39−2.55	2.4; 4.0	2.1−2.4	2.0−2.5
H_{guest}	3.87	3.4	3.4−4.1	3.0−3.4

[a] ^{1}H solution state NMR chemical shifts were obtained from the $\Delta\delta_{max}$ values determined in titration experiments. [b] GIAO-HF/TZP//HF/6-31G*. [c] GIAO-HF/TZP + Δ_{Di}^{SVP} + Δ_{Tri}^{3-21G}// HF/6-31G*. [d] GIAO-HF/TZP + Δ_{Di}^{SVP}// HF/6-31G*. [e] GIAO-HF/6-31G*//HF/6-31G*.

3. NMR Results

3.1. One-Dimensional ^{1}H NMR Experiments. From the consideration alone of the chemical structure of the isolated molecules that make up the complexes, it would be expected that the ^{1}H solid-state NMR spectra exhibit a prominent peak at about 7 to 8 ppm due to the tweezer aromatic protons, together with two resonances for the methylene protons and the "bridgehead" protons of the norbonadiene units at about 2.5 and 4.1 ppm, respectively (as based on the solution-state data). The guest molecules, having only two (TCNB) or four protons, are expected to only marginally affect the overall ^{1}H MAS spectrum.

In Figure 2, the ^{1}H MAS spectra of the three complexes are shown. Using an MAS frequency of 30 kHz, the spectral resolution is sufficient to observe distinct resonances. In all spectra, the resonances due to the aromatic host protons are observed but also note significant differences in the range between 0 and 5 ppm with various overlapping resonances. These differences illustrate that the influence of the guest molecules on the chemical shifts of *all* protons might be larger

(77) Gullion, T.; Schaefer, J. *J. Magn. Reson.* **1989**, *81*, 196.
(78) Kong, J., et al. *J. Comput. Chem.* **2000**, *21*, 1532−1548.
(79) Ahlrichs, R.; Michael, B.; Haeser, M.; Horn, H.; Kölmel, C. *Chem. Phys. Lett.* **1989**, *162*, 165−169.
(80) Ochsenfeld, C.; White, C. A.; Head-Gordon, M. *J. Chem. Phys.* **1998**, *109*, 1663−1669.
(81) Ochsenfeld, C. *Chem. Phys. Lett.* **2000**, *327*, 216−223.
(82) White, C. A. J.; Benny G.; Gill, Peter M. W.; Head-Gordon, Martin *Chem. Phys. Lett.* **1994**, *230*, 8−16.
(83) Shao, Y. H.; White, C. A.; Head-Gordon, M. *J. Chem. Phys.* **2001**, *114*, 6572−6577.
(84) London, F. *J. Phys. Radium* **1937**, *8*, 397.
(85) Ditchfield, R. *Mol. Phys.* **1974**, *27*, 789−807.
(86) Wolinski, K. H.; James F.; Pulay, Peter *J. Am. Chem. Soc.* **1990**, *112*, 8251−8260.
(87) Haeser, M. A.; R.; Baron, H. P.; Weis, P.; Horn, H. *Theor. Chim. Acta* **1992**, *83*, 455−70.

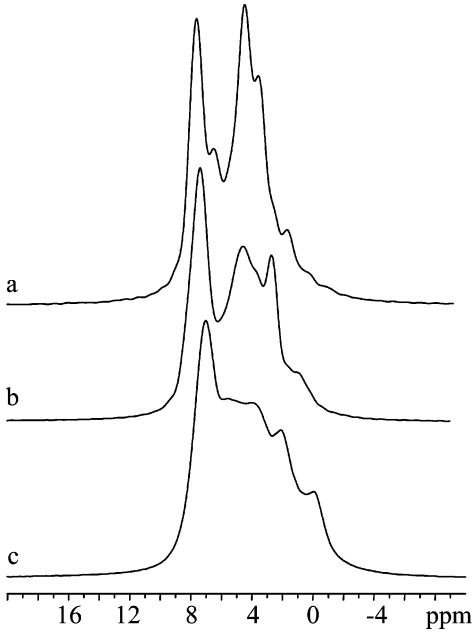

Figure 2. ^{1}H MAS NMR spectra of the complexes formed by the tweezer and (a) TCNQ, (b) TCNB, and (c) DCNB.

than one would expect at first glance. In order to assign the resonances properly, two-dimensional methods are needed to establish (a) correlations between the observed ^{1}H resonances and (b) connectivities to the carbons of the host and guest molecules.

3.2. Complexes with TCNB and DCNB. As noted above, the complex formed with DCNB was the subject of detailed NMR experiments and quantum-chemical calculations of the ^{1}H and ^{13}C chemical shifts.[63,64] As seen in Figure 3, the structure of the complex with TCNB is very similar to that of the DCNB complex: the tweezer geometry in the complex differs only marginally and the TCNB molecule has almost the same position inside the tweezer cavity as DCNB. In the case of TCNB, the distance (determined by X-ray diffraction) between the centers of the guest benzene and host naphthalene units is 0.335 nm (DCNB: 0.375 nm), while the guest protons are 0.244 nm (DCNB: 0.253 nm) apart from the next host arene unit (see also Figure 9). Owing to these similarities, a direct comparison between these two complexes and their spectra will help us to assign the resonances found in the one- and two-dimensional spectra.

In a rotor-synchronized ^{1}H DQ MAS spectrum for the TCNB complex (see Figure 4), three distinct pairs of cross-peaks are resolved, with the one-dimensional spectra a−c representing slices through the two-dimensional spectrum at DQ frequencies of (a) 2.0 + 4.1 = 6.1 ppm, (b) 2.0 + 7.0 = 9.0 ppm, and (c) 4.1 + 7.0 = 11.1 ppm. The latter might overlap with a further correlation between the resonances at 7.0 and 5.0 ppm as seen in slice (b) for the complex with DCNB, where clear correlation peaks are also observed at 5.6 and 2.0 ppm (see slice (a)). In both spectra, an autocorrelation peak for the aromatic protons of the tweezer at 7.0 ppm is apparent.

Correlation (c) for the complex with TCNB is assigned to the expected intramolecular proximities within the tweezer molecules: the protons of an arene unit are dipolar coupled to the "bridgehead" protons. For example, this correlation represents the spatial proximity of H^1 and H^4 with H^{24} and H^5, respectively. For the complex with DCNB, the resonances at 5.6 and 2.0 ppm have been shown to correspond to the two nonequivalent protons of the guest molecule.[64] An inspection of the spectrum for the complex with TCNB reveals that both slices (a) and (b) show a resonance at 2.0 ppm which, as in the DCNB complex, can be tentatively assigned to the TCNB guest protons (pointing to the tweezer sidewalls).

Owing to the improved spectral resolution of the DQ MAS spectrum at least five resonances are identified, but it should be kept in mind that even under fast MAS further signals are likely to be hidden due to the considerable residual line widths. In order to unambiguously assign the resonances, a comparison with results from ^{1}H solution state NMR shows only agreement for the resonances at about 7.0 and 4.0 ppm assigned to the aromatic and the "bridgehead" protons of the tweezer, respectively. However, in the solution state NMR spectrum, no resonances at 5.0, 5.6, and 2.0 ppm were observed[18] rendering the interpretation of the correlation peaks and of one diagonal peak more difficult.

Therefore, ^{1}H−^{13}C correlation experiments were performed to identify the corresponding directly bonded carbon resonances, thus allowing the unambiguous assignment of the proton resonances. The advantage of such a heteronuclear experiment is the inherent smaller line width and greater range of chemical shifts for the ^{13}C resonances resulting in an improved spectral resolution. Second, for small and medium sized molecules the ^{13}C chemical shifts do not differ significantly (as compared to the range of observed chemical shifts) in the solid state and in solution facilitating the assignment. In this way, the ^{1}H chemical shifts can be resolved and assigned. A recoupled polarization transfer heteronuclear single-quantum correlation experiment (^{1}H−^{13}C REPT-HSQC)[76] was applied which uses a REDOR-type pulse sequence for the ^{1}H−^{13}C polarization transfer and fast MAS to achieve sufficient resolution in the ^{1}H dimension. The spectra obtained for the DCNB and TCNB complexes are depicted in Figure 5. Consider first the aromatic carbon atoms: for the complex with DCNB, two correlation peaks (marked with A) at a ^{13}C chemical shift of about 130 ppm and ^{1}H chemical shifts of 2.0 and 5.6 ppm are observed − these have been assigned to the protons a (2.0 ppm) and b (5.6 ppm) of 1,4-dicyanobenzene.[64] Obviously, in the solid state, these two protons are not equivalent suggesting a fixed position of the guest molecule within the cavity of the tweezer.

Analogously, in the spectrum of the TCNB complex, the proton and CH carbon atom of tetracyanobenzene are identified by the correlation peak A′ at 133.4 (^{13}C) and 1.9 ppm (^{1}H). The aromatic protons of TCNB pointing toward the tweezer sidewalls again show a remarkable high field shift due to the ring current of the arene units of the tweezer. This finding is consistent with the crystal structure of the complex (see Figure 3).

In the solution state NMR spectra[18] the carbon resonances below 129 ppm were assigned to carbon atoms of the tweezer (see also Supporting Information). Interestingly, three correlation peaks are observed for these aromatic carbon atoms in the ^{13}C−^{1}H correlation spectra of both complexes. Two of these peaks appear at a ^{1}H chemical shift of 6.8−7.2 ppm, but one (marked with B and B′, respectively) is found at about 5.0 ppm. This particular resonance is in agreement with the correlation peak

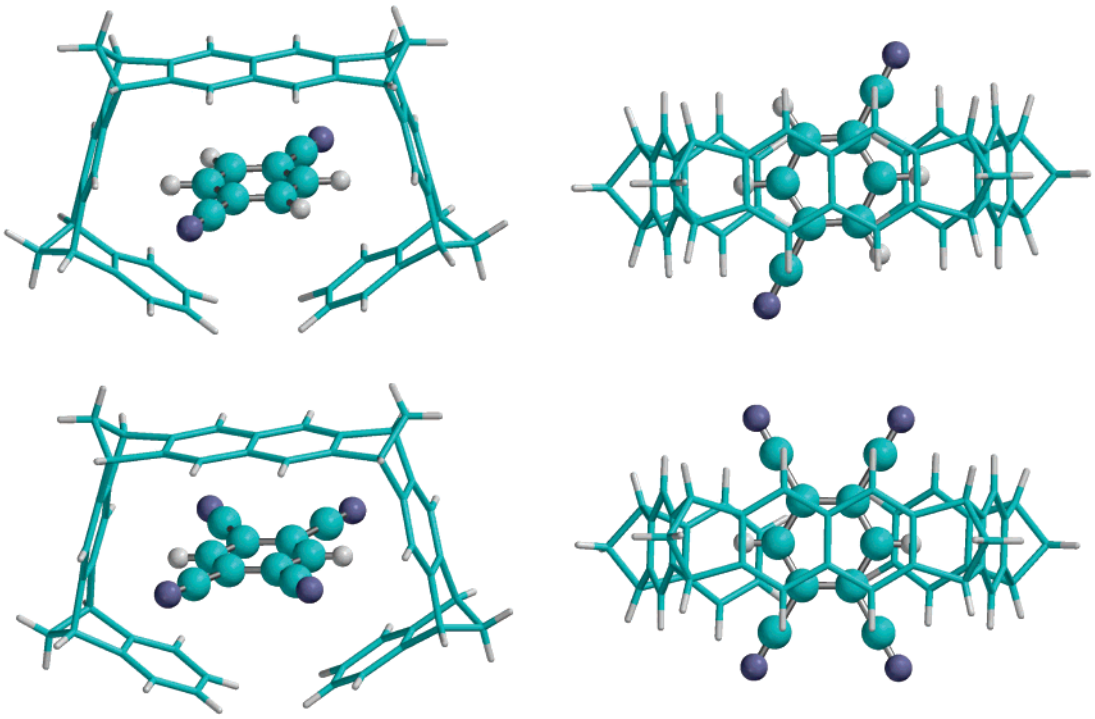

Figure 3. Complex (top) with 1,4-dicyanobenzene (DCNB: $H_{guest,a}$, $H_{guest,b}$ point toward the tweezer benzene units of the sidewalls and out of the cavity, respectively) and (bottom) with 1,2,4,5-tetracyanobenzene (TCNB).

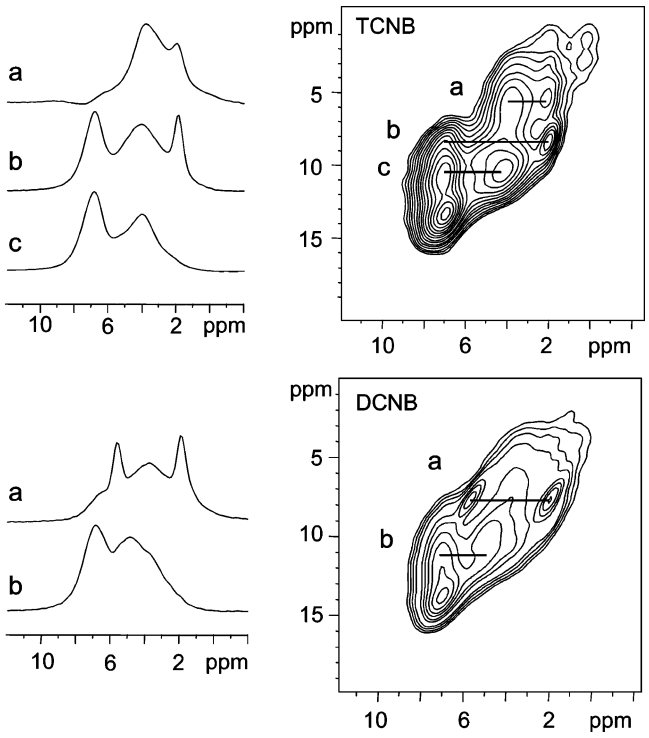

Figure 4. ^{1}H rotor-synchronized DQ MAS spectra of the complexes with (top) 1,2,4,5-tetracyanobenzene (TCNB) and (bottom) 1,4-dicyanobenzene (DCNB). For TCNB, slices (a, b, c) show the correlation peaks between the resonances at (a) 4.1 and 2.0 ppm, (b) 7.0 and 2.0 ppm, and (c) 7.0 and 4.1 ppm, while, for DCNB, slices (a, b) show the correlation peaks between the resonances at (a) 5.6 and 2.0 ppm and (b) 7.0 and 5.0 ppm.

in the ^{1}H DQ MAS spectrum, suggesting that signals of aromatic tweezer protons are also subject to a high-field shift.

A number of correlation peaks are observed in the aliphatic region (40−80 ppm). From solution state NMR, two typical correlations were to be expected and are indeed found: (i) the "bridgeheads" with chemical shifts of 52 and 4.0 ppm, respectively, and (ii) the methylene groups with correlation peaks at about 67 and 2.0 ppm, respectively. In addition, further correlation peaks were detected for the methylene groups with noticeable high field shifts of the proton resonances. In the DCNB complex, this resonance is found at 68.6 and −1.2 ppm (C), whereas, for the complex with TCNB, this resonance is observed at 64.6 and −0.2 ppm (C′). It should be noted that the intensity of the methylene signals, however, is small compared to the peaks of the bridgeheads, with it having been noted that the single-quantum coherences of CH_2 groups tend to relax very fast resulting in a significant loss of intensity or, in some cases, even the loss of this particular signal.[76]

In summary, it is possible to identify the protons of the guest molecule as well as observe ^{1}H resonances for protons of the tweezer with unexpected chemical shifts presumably due to the ring currents due to adjacent arene units. Given the absence of such resonances in the solution state, this effect must be assigned to the specifics of a solid, i.e., to the arrangement of the complexes within the crystal lattice. This assumption is confirmed by the single-crystal structure analysis of these complexes.

Figure 6 shows the arrangement of the tweezer complexes with DCNB[18] and TCNB in the crystal lattice. The DCNB complexes form two columns which are shifted by about half the size of one complex. This arrangement leads to a rather dense packing resulting in short distances between adjacent supramolecules. As expected, the shortest proton−proton distance is found within the cavity: H^a of DCNB is only 0.253 nm apart from the center of the next benzene ring of the tweezer resulting in the observed chemical ^{1}H NMR shift of 2.0 ppm (correlation peak A in Figure 5). Besides this "intramolecular" interaction, close proximities between tweezer protons and neighboring arene units are found. Within one column, the

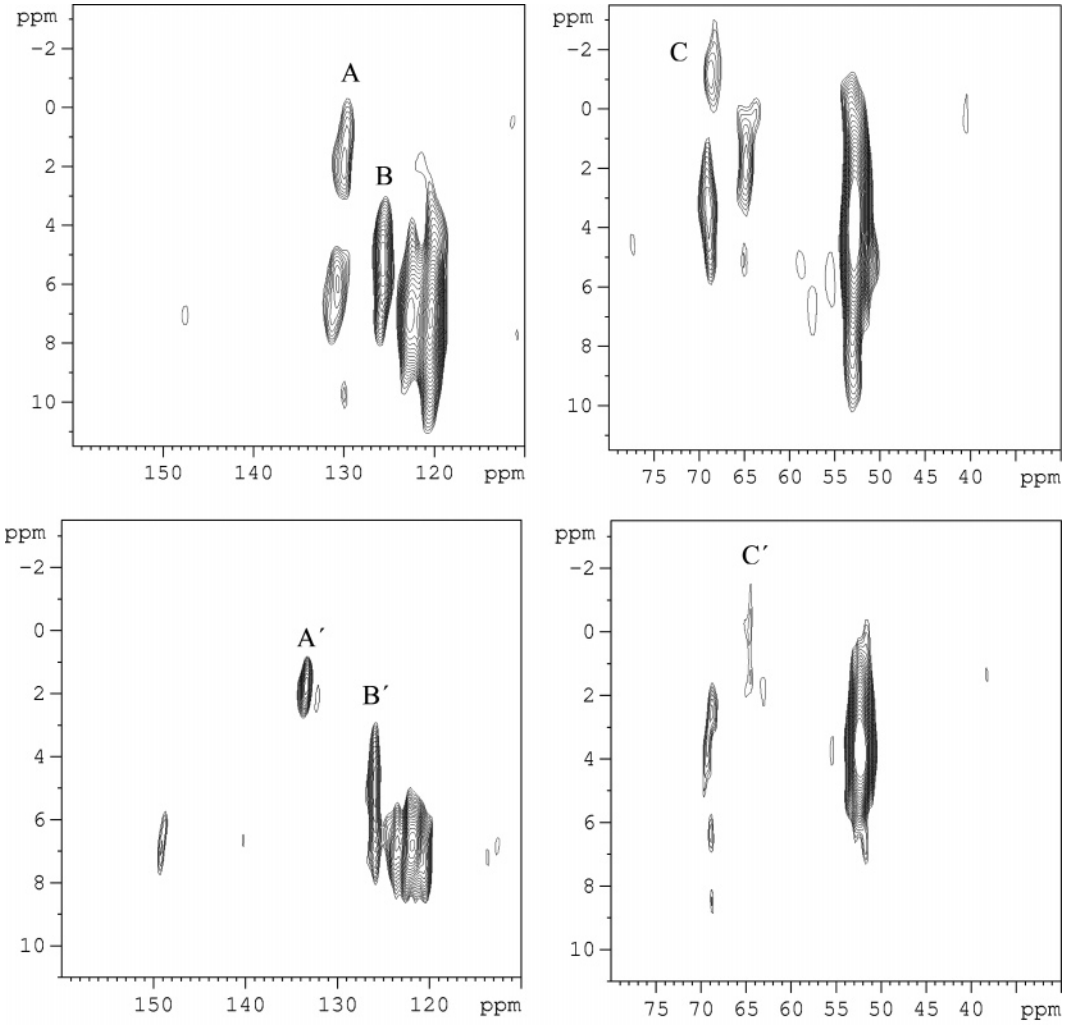

Figure 5. ^{1}H rotor-synchronized $^{1}H-^{13}C$ REPT-HSQC spectra of the complex with (top) 1,4-dicyanobenzene (DCNB) and (bottom) 1,2,4,5-tetracyanobenzene (TCNB); the spectra on the left and right correspond to the aromatic and aliphatic carbon atoms, respectively.

protons of the tweezer "tip" (i.e., H^1, H^2, H^{14}, H^{15}, see Supporting Information) approach the central naphthalene unit of the next tweezer; the distance to the closest benzene ring is 0.344 nm, thus indicating that resonance B at about 5.0 ppm is to be assigned to these protons. Furthermore, the next column of complexes affects the methylene protons: the distance of the methylene protons to the terminal or middle benzene ring of the neighboring complex ranges from 0.280 to 0.426 nm. This close proximity results in the high-field shifted correlation peak C.

A similar packing scheme is obtained for the complexes with TCNB; again, two columns with the tweezer tips heading in opposite directions are arranged in such a way that a very close packing is achieved. The closest distances are those between the guest proton and a benzene unit ($d_1 = 0.244$ nm); thus, the observation of an upfield shifted correlation peak A′ is not surprising.

Resonance B′ is due to tweezer tip protons which are only 0.355 and 0.325 nm away from the next naphthalene spacer unit (d_2). The methylene protons have a distance of 0.276 nm (d_3) and 0.463 nm (d_4) to the arene units of the adjacent tweezer resulting in the correlation peak C′.

3.3. Complexes with TCNQ. The crystal structure of the complex with TCNQ (see Figure 7)[18] differs from the supramolecules discussed above: although a symmetrical guest molecule is complexed, the host is significantly deformed resulting in a loss of internal symmetry and an increase in the number of nonequivalent proton and carbon positions. For example, four different distances between the nonequivalent guest protons and the center of the middle benzene ring (0.285, 0.312, 0.314, and 0.307 nm, respectively) are observed.

In the ^{1}H DQ MAS spectrum (see Figure 8) of the complex with TCNQ, while an autocorrelation peak of the aromatic tweezer protons was again detected, a second diagonal resonance was observed at 4.0 ppm. In addition, correlations between nonequivalent protons are observed as cross-peaks at (a) 7.2 + 3.2 = 10.4 ppm, (b) 7.2 + 4.1 = 11.3 ppm, and (c) 7.2 + 6.0 = 13.2 ppm. While correlation (b) is the same as in the other two complexes, (a) and (c) are new.

In the $^{1}H-^{13}C$ REPT-HSQC spectrum of the TCNQ complex (Figure 9), the main difference to the $^{1}H-^{13}C$ REPT-HSQC spectra in Figure 5 is the reduced high field shift of all protons for which a marked sensitivity to ring currents was observed above. The guest protons can be assigned by their correlation peak A″ at 128 (^{13}C) and 3.3 ppm (^{1}H); interestingly, only one resonance is observed. This can be explained either by equivalent environments or by a fast reorientation of the guest molecule resulting in an averaged ^{1}H resonance. The

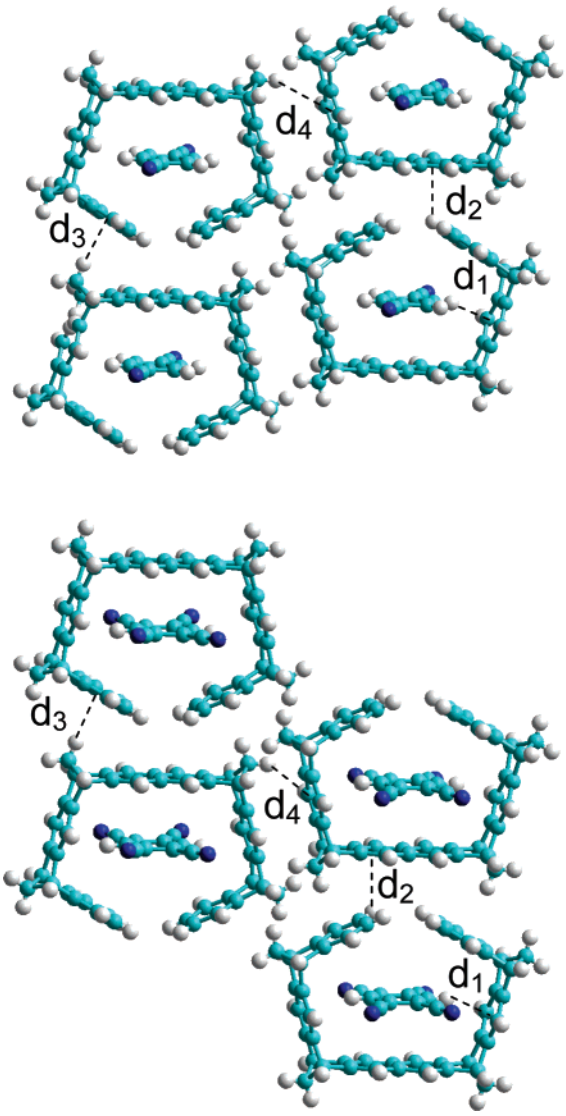

Figure 6. Crystal packing structure of the complexes with DCNB (top) and TCNB (bottom). In the case of DCNB, the shortest distances between protons and the center of the next benzene ring are $d_1 = 0.253$ nm, $d_2 = 0.344$ nm, $d_3 = 0.280$ nm, and $d_4 = 0.426$ nm. For TCNB, the indicated distances are $d_1 = 0.244$ nm, $d_2 = 0.314$ nm, $d_3 = 0.280$ nm, and $d_4 = 0.463$ nm.

high-field shifted aromatic protons are identified by a correlation peak B″ with rather low intensity at 125 ppm (^{13}C) and 6.0 ppm (^{1}H).

Besides the intense correlation peak of the bridgehead protons, only weak peaks were detected for the methylene groups showing no (^{1}H chemical shift of 2.2 ppm) or only a small high-field shift (^{1}H: 1.0 ppm, C″) analogous to the small shift of the aromatic host protons.

This result indicates a very different packing scheme of the complexes with TCNQ in the crystal lattice (Figure 10) compared to both of the other complexes discussed above. Due to the sterically more demanding guest a columnar arrangement of the complexes is prevented which leads to larger distances between the supramolecules. In addition, the complexes are twisted relative to each other. Due to the arrangement of the complexes, the distances of the methylene protons to arene units of the next complex are increased to at least 0.35 nm. The terminal benzene protons have a distance of at least 0.340 nm

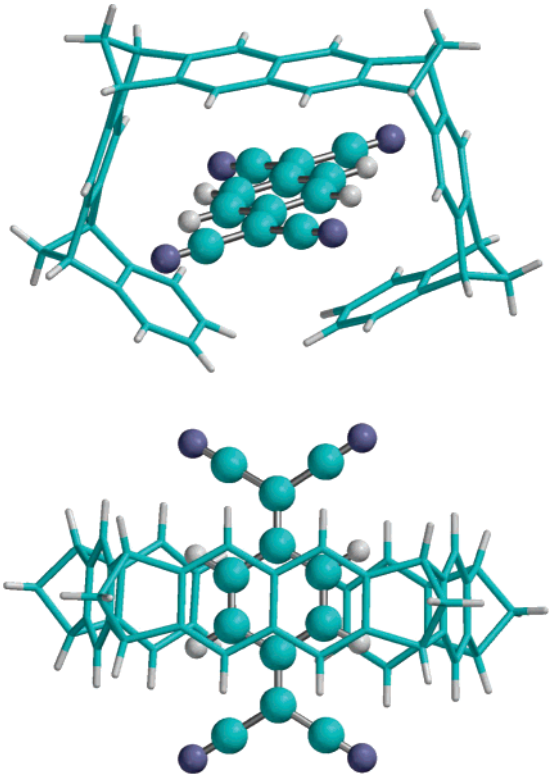

Figure 7. Crystal structure of the complex with 7,7,8,8-tetracyano-*p*-quinodimethane (TCNQ).

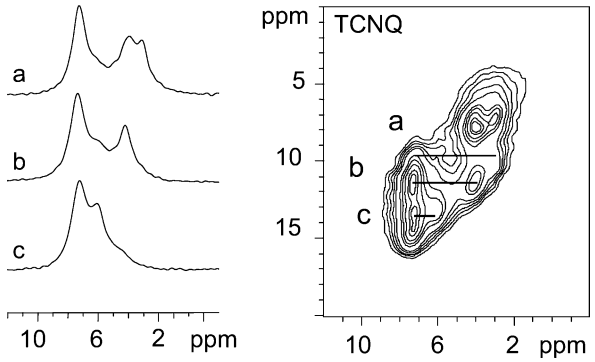

Figure 8. ^{1}H rotor-synchronized DQMAS spectrum of the complex with 7,7,8,8-tetracyano-*p*-quinodimethane (TCNQ) and slices (a, b, c) corresponding to correlation peaks between the resonances at (a) 7.2 + 3.1 = 10.3 ppm, (b) 7.2 + 4.2 = 11.4 ppm, and (c) 7.2 + 6.0 = 13.2 ppm.

to the next arene unit. Thus, in the crystalline TCNQ complex, smaller intermolecular C−H - - - π interactions are expected than in the crystalline DCNB or TCNB complex. As a consequence, smaller high field shifts for the protons of the tweezer—aromatic protons (correlation peak B″) and methylene protons (C″) as well—are to be expected for the TCNQ complex which is qualitatively in agreement with the experimental results.

In order to verify the qualitative interpretation of intramolecular C−H - - - π interactions and crystal packing effects, quantum chemical calculations were applied for all three complexes discussed above.

4. Quantum Chemical Calculations

In such supramolecular systems, the combination of quantum chemical calculation of NMR shifts with experimental data has been established as a method of structure analysis.[22,63,64,88] The

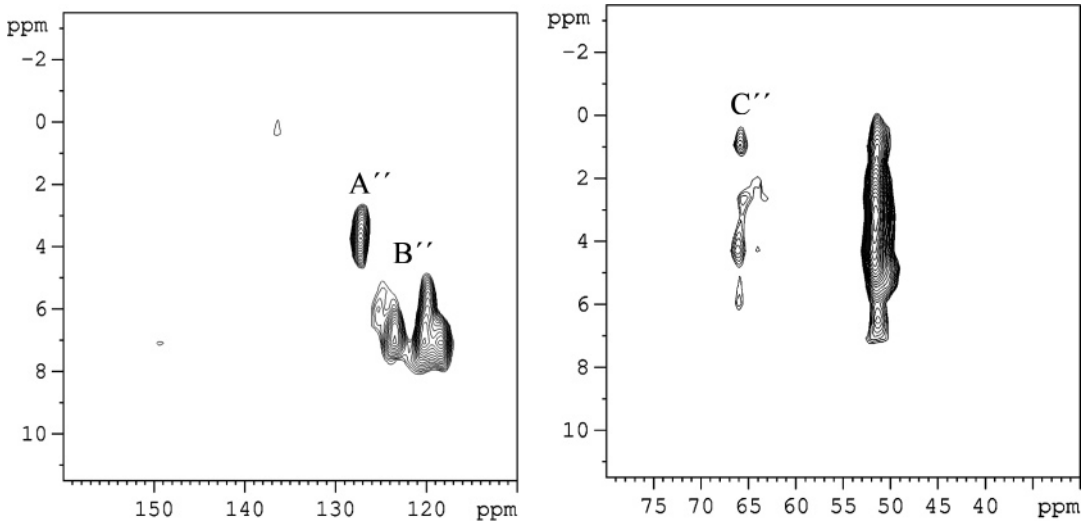

Figure 9. $^{1}H-^{13}C$ rotor-synchronized $^{1}H-^{13}C$ REPT-HSQC spectrum of the complex with 7,7,8,8-tetracyano-*p*-quinodimethane (TCNQ); the left and right spectra correspond to the aromatic and aliphatic carbon resonances, respectively.

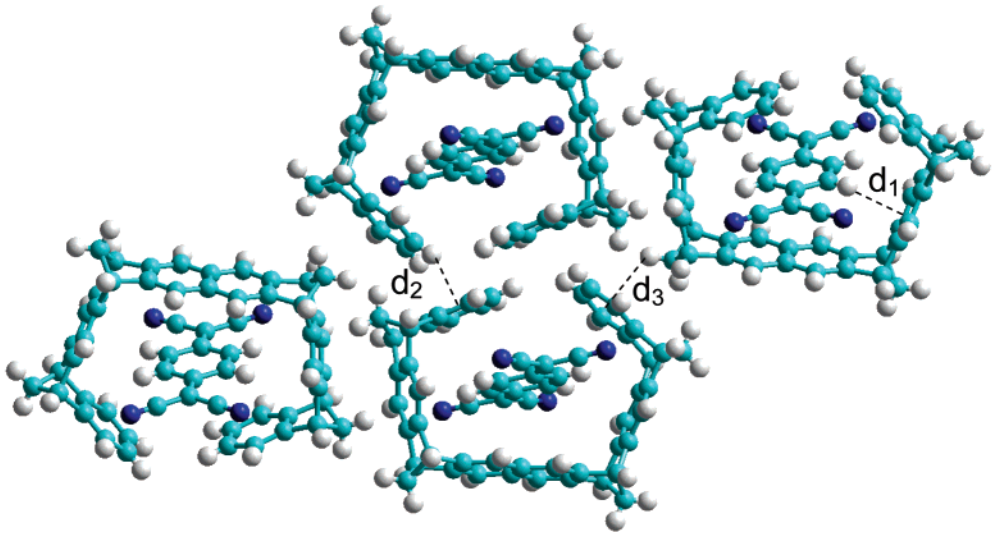

Figure 10. Crystal packing structure of the complex with TCNQ; d_1 ranges from 0.285 to 0.307 nm (see section 3.3), $d_2 = 0.340$ nm, and $d_3 = 0.350$ nm.

complex with DCNB has been the subject of detailed investigations;[63,64] here, we focus on the complexes with TCNB and TCNQ and summarize the results of all three host−guest systems in Table 1.

In order to compute the ^{1}H NMR spectrum of the TCNB host−guest complex, the starting point was the optimization of the structure at the HF/6-31G* level using constraints for positioning the guest molecule within the host. As shown earlier for substituted hexabenzocoronenes,[61] it is not possible to use directly the X-ray structure data for the NMR shift calculations since in the experiment the proton positions are not resolved, but instead empirically added, so that they do not correspond to a relaxed electronic structure. For the structure optimization additional constraints have been introduced in order to take into account influences exerted by neighboring complexes within the solid state as well as to avoid problems by missing dispersion type interactions within the HF approach. As constraints we have used the distances C2−C15, C3−C14, C5−C12, C17−C24, C8a−Cb, C8a−Cb′, C20a−Cb″, and C20a−Cb‴ (Supporting information) from the X-ray data. A dimer fragment was then constructed by translating the optimized host−guest complex using the X-ray distance of atom C20a as a reference.

Using the optimized structure, the NMR chemical shifts for the monomer were computed at the GIAO-HF/TZP level. For the dimer fragment, the shieldings were calculated within an incremental scheme described earlier:[64] the two units A and B of a dimer influence each other describing the interactions occurring in the full solid-state structure. Therefore, we consider the changes of both A and B with respect to the monomer chemical shifts at the same level of theory. These dimer contributions computed at the GIAO-HF/SVP level are then added to the monomer chemical shifts (GIAO-HF/TZP) and result in the final estimate for the dimer chemical shifts.

The data for the monomer and the dimer listed in Table 1 show a good agreement between experiment and theory, while the error bars of both the solid-state NMR experiment as well as of the GIAO-HF calculations are typically in the order of 0.2−0.5 ppm. Here, the computed monomer data can be compared to the solution state NMR experiment, while for comparison with the solid-state NMR experimental data it is

(88) Klarner, F. G.; Kahlert, B.; Nellesen, A.; Zienau, J.; Ochsenfeld, C.; Schrader, T. *J. Am. Chem. Soc.* **2006**, *128*, 4831−4841.

necessary to resort to a dimer at least. This becomes particularly clear in considering the chemical shift of $H_{arom,term}$ of 6.6 ppm for the monomer, which changes in the dimer to 4.9 ppm which is now in perfect agreement with the experimental MAS NMR value of 4.9 ppm.

The structure optimization for TCNQ was performed in analogous fashion to that for TCNB. As constraints the distances C5−C12, C17−C24, C20a−Ca, C20a−Cb, C8a−Ca′, C8a−Cb′, C3−C14, C2−C15 were used. To account for the distorted shape of the tweezer, the C−16−19−22−1, C−13−10−7−4 torsion angles were also restrained. For the projection onto the X-ray structure, all guest C atoms were used as well as the C atoms 1, 2, 8a−12a, 9−14, 21a−24a, 21−24 of the tweezer.

Since the X-ray structure is more complicated than for the other host−guest complexes, we reverted to a pentamer fragment as a minimal unit for describing the solid-state behavior. As a first approach for estimating the influences onto the central host−guest complex of the pentamer fragment, we employed an incremental approach describing the influences by two trimer units, with this being similar to the approach we used for the DCNB and TCNB guests.

Here, the influence of the two upper host−guest complexes on the central one and of the two lower complexes onto the central unit is considered. These values were computed at the GIAO-HF/3-21G level and then added to the GIAO-HF/TZP monomer values. In order to check this incremental scheme previously employed,[64] our new linear-scaling method now permits the computation of the full pentamer both at the GIAO-HF/3-21G and at the GIAO-HF/6-31G* level.[65] The comparison of the data for the pentamer obtained at the GIAO-HF/3-21G level within either the incremental trimer scheme or the full direct calculation revealed differences of less than 0.3 ppm, indicating the usefulness of this approach.

Nevertheless, since we are now able to compute the entire pentamer we can avoid the incremental approach and perform the calculation for the 490 atom systems denoted as pentamer at the GIAO-HF/6-31G* level. The corresponding data are listed in Table 1. The agreement in comparing the solution state experiment to the computed monomer values and the solid-state NMR data to the computed pentamer values is mostly within the error bars of experiment and theory. The only large deviation upon comparing the solid-state NMR experiment and the pentamer calculations is 1.0−1.6 ppm for the aromatic protons of the tip of the tweezer (denoted as $H_{arom,term}$). The reason for this discrepancy may be that it would be necessary to consider an even larger fragment; this needs to be further investigated in future studies. As for the guest protons the agreement between experiment and theory is within 0.5 ppm for the solution spectrum and within 0.4 ppm for the solid-state NMR data. The relatively small change between the experimental values in solution and in the solid state of 0.5 ppm shows a relatively small influence of the different environments onto the guest bound within the clip.

5. Summary and Conclusions

In most of the investigations on supramolecular complexes, solution state NMR experiments have been applied that provide a time-averaged picture of such host−guest systems. In contrast solid-state NMR experiments allow the direct observation of host−guest complexes for the specific cases considered here of the naphthalene tweezer with DCNB, TCNB, and TCNQ; due to the greater complexity in the solid-state NMR spectra resulting from the crystal lattices, input from quantum chemical calculations is needed for the interpretation of the NMR results.

For all three complexes studied here, single-crystal data were available providing a structural basis for the calculation of ^{1}H chemical shifts. As seen in Table 1, the chemical shifts calculated for the guest protons in an isolated complex are in good agreement with the experimental data. However, in order to obtain a similar precision for the ^{1}H chemical shifts of the host protons, larger fragments need to be taken into account. For the structurally similar complexes with DCNB and TCNB, the influence of neighboring complexes on the chemical shifts was calculated and added to the data of a monomeric unit. With such an incremental approach the calculated ^{1}H chemical shifts of the tweezer protons were well in accord with the solid state ^{1}H NMR results. This method was also used for the complex with TCNQ where even four neighboring complexes contributed to the calculated chemical shift. This pentamer (with 490 atoms) is one of the first complex systems to which the recently introduced linear-scaling NMR method has been applied.[65] With the new methods combined with increasing capabilities of computational hardware, calculations for systems with more than 1000 atoms become possible, although, in the case of the naphthalene tweezer complexes, the comparison with the incremental approach also shows the validity of the incremental scheme.

The structure of the three complexes and their spatial arrangement in the crystal lattice show remarkable differences. While the complexes with DCNB and TCNB are similar in their packing scheme, the TCNQ complexes are arranged in such a way that intermolecular interactions (such as ring current effects due to neighboring complexes) are reduced resulting in smaller complexation-induced chemical shifts of the host protons.

Comparing the DCNB and the TCNB complexes, the spatial arrangement of the complexes and the position of the guest molecule within the cavity are very similar. It has been shown that the reorientation of the DCNB molecule (180° flip) can be monitored in ^{1}H DQMAS spectra due to the exchange between the two nonequivalent proton positions of DCNB, H_a and H_b. In the TCNB complex, such dynamics would transfer chemically equivalent protons to each other; hence, this molecular motion is not observable in ^{1}H DQMAS spectra. However, if the tweezer is substituted, for example, by OAc groups attached to the central naphthalene spacer unit, the two protons of TCNB become nonequivalent.[24] Consequently, molecular dynamics of the guest molecule within the host cavity can be investigated. Further work along this line is currently in progress.

Furthermore, also host−guest complexes of molecular clips with three or two methylene bridges[21] come into focus. Both investigations on crystal packing effects as well as molecular dynamics could provide a more comprehensive picture of this class of supramolecular complexes in the solid state.

The general approach to combine X-ray diffraction, solid-state NMR, and quantum chemical calculations has numerous potential applications. Investigations on amino acids[89] and small peptides[90] and studies on conformational polymorphism in

(89) Gervais.; C.; Dupree, R.; Pike, K. J.; Bonhomme, C.; Profeta, M.; Pickard, C. J.; Mauri, F. *J. Phys. Chem. A* **2005**, *109*, 6960−6969.
(90) Cheng, F.; Sun, F.; Zhang, Y.; Mukkamala, D.; Oldfield, E. *J. Am. Chem. Soc.* **2005**, *127*, 12544−12554.

pharmaceutical solids[91,92] are the first examples of a rapidly developing field which is expected to extend to more complex and biologically relevant systems.

Even in cases where no crystal structure data are available, NMR experiments and quantum chemical calculations provide complementary information: solid-state NMR results have been shown to provide valuable constraints for quantum chemical calculations which allowed the determination of packing arrangements.[62] Also in solution, ab initio calculations are necessary to interpret the results from NMR results on complex systems.[88]

(91) Hughes, C. E.; Olejniczak, S.; Helinski, J.; Ciesielski, W.; Repisky, M.; Andronesi, O. C.; Potrzebowski, M. J.; Baldus, M. *J. Phys. Chem. B* **2005**, *109*, 23175−23182.
(92) Smith, J. R.; Xu, W.; Raftery, D. *J. Phys. Chem. B* **2006**, *110*, 7766−7776.

Acknowledgment. This work has been supported by the Deutsche Forschungsgemeinschaft (SFB 452 and SFB 625). C.O. acknowledges financial support by an Emmy Noether research grant of the DFG. S.P.B. thanks the EPSRC for the award of an Advanced Research Fellowship.

Supporting Information Available: Solution and solid-state NMR chemical shifts; quantum-chemical calculations of the ^{1}H NMR chemical shifts for the host−guest complexes of the naphthalene tweezer with DCNB, TCNB, and TCNQ, respectively; and complete citation of ref 78. This material is available free of charge via the Internet at http://pubs.acs.org.

JA0666351